

Reliability-based MCDM Using Objective Preferences Under Variable Uncertainty

Deepanshu Yadav¹[0000-0003-1841-8942], Palaniappan Ramu¹[0000-0001-9704-2087], and Kalyanmoy Deb²[0000-0001-7402-9939]

¹ Indian Institute of Technology Madras, Chennai, India

² Michigan State University, East Lansing, USA

deepanshu.yadav380@gmail.com, palramu@iitm.ac.in, kdeb@egr.msu.edu

COIN Report Number 2024009

Abstract. The state-of-the-art evolutionary algorithms (EAs), developed to solve constrained multi/many-objective optimization problems (M/MaOPs), mostly deal with deterministic design variables causing no uncertainty in their implementation. However, from a practical point of view, it is imperative to consider unavoidable uncertainties in implementing design variables and parameters. In the presence of hard constraints, a slight change in one or more variables may cause a feasible optimal solution to become infeasible upon implementation and result in a failure during operation. The literature suggests reliability-based techniques for solving such M/MaOPs to obtain a *Reliable Front* (ReF), rather than a Pareto-optimal front (PF). A ReF is usually either a part of the PF or a completely different set of trade-off solutions dominated by the deterministic PF. However, in the presence of decision-making, computing the complete ReF may not be necessary, as the focus would be to locate only the preferred part of the ReF, dictated by the objective preference information by a decision-maker (DM). The proposed approach incorporates DM's preferences and variable uncertainty information a priori. The proposed Reliability-based Multi-criteria Decision-making (ReMCDM) approach uses the hybrid mean value (HMV) method for constrained handling under variable uncertainties and R-NSGA-III for preference incorporation by DMs to conduct MCDM. Results obtained by the proposed method, implemented on several benchmark and real-world engineering examples, encourage future EMO research combining constraint handling, uncertainty in decision variables, and preference incorporation.

Keywords: Evolutionary Algorithms · Multi-objective Optimization · Reliability · Preference Incorporation · Decision-making.

1 Introduction

Real-world applications generally deal with multiple and conflicting objectives [3]. In literature, these applications are treated as multi-objective optimization (MOO) problems [30,6]. The outcome of optimizing an MOO problem is not a

unique solution but is a set of non-dominated (ND) solutions, located near the Pareto front (PF) [23]. PF is a set of optimal solutions in objective space such that improvement in one objective is only possible upon sacrificing at least one other objective [7]. Evolutionary multi-objective optimization (EMO) algorithms such as NSGA-II [11], NSGA-III [14], RVEA [4], C-TAEA [19], and MOEA/D [45] among others, are developed to compute a set of ND solutions close to PF in a single computational effort. However, from a practical point of view, the decision maker (DM) has to pick one or a few solutions lying on PF by discarding other solutions [2]. As computing the complete PF is computationally costly, Multi-criteria Decision-making (MCDM) techniques are developed in the literature to incorporate DM's preferences to arrive at a part of PF satisfying the aspiration level of DM. These MCDM algorithms include R-NSGA-II [12], RD-NSGA-II [10], R-NSGA-III [32], *g*-NSGA-III [25], light beam search [9,15], and other scalarization-based approaches [24].

In practical implementation, variable uncertainty is unavoidable in design and optimization [26]. These uncertainties are inevitable and come from different sources including process parameters, manufacturing tolerances, instrument precision, measurement errors, etc. Therefore, it is crucial to consider variable uncertainty in M/MaOPs. Singh and Branke [29] proposed evaluating the non-dominated solutions in stochastic decision variables. For constrained M/MaOPs, usually, the optimal solutions lie on constraint boundaries(s) [28,13]. In such scenarios, uncertainty in design variables may also lead to an infeasible solution(s) causing design failure. Hence, constraint handling under variable uncertainty needs a different treatment than that in a regular MOO formulation, to provide reliable solutions such that the probability of design failure due to constraint violation is very low. Reliability-based design optimization (RBDO) methods [42,1] are developed to account for such problems. In RBDO, double-loop approaches (DLA) are popular. In a DLA, the outer loop searches for optimal design variables by solving the regular optimization problem, and in the inner loop the reliability index [8] at a design solution is calculated to evaluate the solution's reliability against constraint violation or failure.

Reliability estimation methods include sampling-based and optimization-based approaches. The literature on sampling-based approaches is provided in [17,27,39]. Optimization-based techniques include first-order reliability methods (FORM) such as the Reliability Index Approach [5] and the Performance Measure Approach [43], which computes Most Probable Target Point. The Advanced Mean Value method [33], Conjugate Mean Value method [44], and Hybrid Mean Value method [16] were proposed in the literature to compute Most Probable Target Point (MPTP). The limitations of these methods were addressed by Chaos Control theory-based methods [40], the Modified Chaos Control method [20], and Adaptive Chaos Control method [18]. The relevant literature on reliability-based design optimization can be found in [8,21,22]. It is to be noted that computing ReF is computationally expensive [8]. We propose using the Reference point based-EMO (R-EMO) algorithm to compute part of ReF using the optimization formulation provided in Equation 2. The proposed ap-

proach is termed as reliability-based MCDM (ReMCDM). ReMCDM uses DLA, in which the outer loop solves the original optimization problem (in Equation 1) using R-NSGA-III. Hybrid Mean Value method accounts for constraint (in Equation 2) handling under variable uncertainty and reliability estimation in the inner loop. This approach avoids computing the complete PF or ReF.

The rest of the paper is organized as follows: Section 2 provides details on constraint handling under variable uncertainty in the context of MOO. Section 3 outlines the proposed approach for ReMCDM followed by results in Section 4. The conclusions, along with a summary, the limitations of the proposed approach, and directions for future work, are presented in Section 5.

2 Constraint Handling Under Variable Uncertainty

Consider the following /MaOPs formulation [8] provided in Equation 1:

$$\begin{aligned} & \min_{(\mathbf{x}, \mathbf{d})} \left[f_1(\mathbf{x}, \mathbf{d}, \mathbf{p}), f_2(\mathbf{x}, \mathbf{d}, \mathbf{p}), \dots, f_M(\mathbf{x}, \mathbf{d}, \mathbf{p}) \right], \\ & \text{subject to: } g_j(\mathbf{x}, \mathbf{d}, \mathbf{p}) \leq 0, \quad j = 1, \dots, J, \\ & \quad \mathbf{d}^{(lb)} \leq \mathbf{d} \leq \mathbf{d}^{(ub)}; \quad \mathbf{x}^{(lb)} \leq \mathbf{x} \leq \mathbf{x}^{(ub)}. \end{aligned} \quad (1)$$

The problem has M objective functions and J inequality constraints (equality constraints are not considered here for brevity). In Equation 1, \mathbf{x} is the vector of uncertain design variables, \mathbf{d} is the vector of deterministic design variables, which are not uncertain during implementation, and \mathbf{p} is the vector of uncertain parameters, which are not variables of the optimization problem. Figure 1(a) depicts a deterministic optimal solution D obtained at the intersection of two illustrative constraints g_1 and g_2 . Under the variable uncertainty σ_{x_1} and σ_{x_2} , the optimal solution may lie inside the red ellipse. However, many solutions inside the red ellipse do not satisfy the constraint, leaving the optimal solutions infeasible. Hence, there is a probability that the optimal solution under the variable uncertainty becomes infeasible resulting in a design failure. Therefore, constraint handling under variable uncertainty requires a probabilistic MOO formulation to ensure that the probability of design failure does not exceed a pre-specified value (p_f), derived from the desired reliability β . The probabilistic formulation of M/MaOPs, is provided in Equation 2:

$$\begin{aligned} & \min_{(\mu_{\mathbf{x}}, \mathbf{d})} \left[f_1(\mu_{\mathbf{x}}, \mathbf{d}, \mu_{\mathbf{p}}), f_2(\mu_{\mathbf{x}}, \mathbf{d}, \mu_{\mathbf{p}}), \dots, f_M(\mu_{\mathbf{x}}, \mathbf{d}, \mu_{\mathbf{p}}) \right], \\ & \text{subject to: } \Pr(g_j(\mu_{\mathbf{x}}, \mathbf{d}, \mu_{\mathbf{p}}) > 0) \leq p_f, \quad j = 1, \dots, J, \\ & \quad \mathbf{d}^{(lb)} \leq \mathbf{d} \leq \mathbf{d}^{(ub)}; \quad \mu_{\mathbf{x}} \leq \mathbf{x} \leq \mathbf{x}^{(ub)}. \end{aligned} \quad (2)$$

The solution for the optimization problem is the mean value of the uncertain design variable ($\mu_{\mathbf{x}}$) and deterministic design variable (\mathbf{d}). A deterministic constraint in Equation 1 is transformed into a probabilistic constraint in Equation 2. Here, $\Pr(\cdot)$ denotes the probability of failure (or violation of a constraint). The

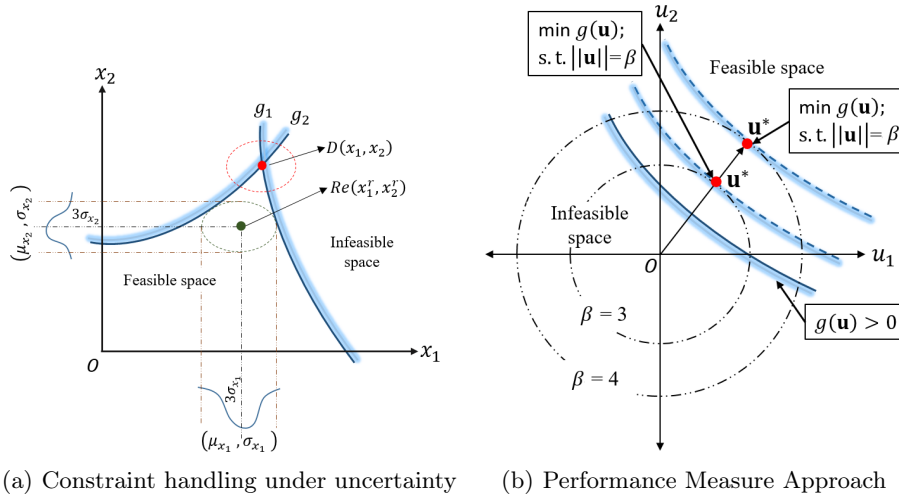


Fig. 1. Reliability-based design optimization: (a) Constraint handling under variable uncertainty for reliability-based design optimization (RBDO). x_1 and x_2 are two design variables. σ_{x_1} and σ_{x_2} are uncertainty associated with them. g_1 , and g_2 are two constraints. D is deterministic solution and Re is reliable solution. (b) Concept of PMA for RBDO. g is a specific constraint and β is target reliability index. u_1 and u_2 are the variables in transformed standard normal space. \mathbf{u}^* (in red dots) is MPTP.

goal of this formulation is to find a reliable point (denoted as Re in Figure 1(a)) inside the feasible space which ensures that in presence of variable uncertainty, the probability of failure is less than or equal to a limit (p_f).

Reliability index β ($= -\Phi^{-1}(p_f)$, where Φ is cumulative standard normal distribution function) of a solution can be approximately computed using Monte Carlo Simulation (MCS) in the vicinity of the solution, but it is a computationally expensive method [42]. Several techniques exist for estimating the β with reduced computational cost, including biased sampling-based methods [27], surrogate models, and extreme-value statistics techniques [17,39]. The other class of approaches uses optimization-based reliability measures. It focuses on identifying the “most probable target point” (MPTP) on the constraint boundary closest to the deterministic solution [8,21]. This approach linearly approximates the constraint near the MPTP to estimate reliability. Due to this linearity assumption, these methods are referred to as first-order reliability methods (FORMs). FORMs include the Performance Measure Approach (PMA) and Reliability Index Approach (RIA). The current work uses PMA approach to compute MPTP for β estimation.

3 Proposed Approach for ReMCDM

The proposed framework uses the double-loop (or bi-level) approach to perform reliability-based MCDM tasks. In the outer loop, the original optimization prob-

lem in Equation 2 is solved using (\mathbf{x}, \mathbf{d}) as design variables. For each (\mathbf{x}, \mathbf{d}) in the outer loop, a chance constraint (involving $\Pr(\cdot)$ in Equation 2) is evaluated in the inner loop using another optimization formulation i.e. PMA or RIA. Instead of solving an M/MaOP to compute the ReF in the outer loop, the proposed method uses preference-based evolutionary multi-objective optimization (R-EMO) algorithms to conduct the MCDM task.

3.1 Performance Measure Approach (PMA)

In PMA at each design point (\mathbf{x}, \mathbf{d}) , the uncertain design variables and uncertain parameters $(\mathbf{v} = (\mathbf{x}, \mathbf{p}))$ are transformed into standard normal space (\mathbf{u}) to arrive at the following optimization formulation:

$$\begin{aligned} & \min_{\mathbf{u}} g_j(\mathbf{d}, \mathbf{u}), \quad j = 1, \dots, J, \\ & \text{subject to: } \|\mathbf{u}\|_2 = \beta, \end{aligned} \quad (3)$$

where $u_k = \frac{v_k - \mu_{v_k}}{\sigma_{v_k}}$, for $k = 1, 2, \dots, K$; K is dimension of the vector space of \mathbf{v} and β is reliability index. After solving the optimization problem in Equation 3, the MPTP solution (\mathbf{u}^*) is obtained at point \mathbf{d} . The obtained \mathbf{u}^* is transformed back to $\mathbf{v}^* = (\mathbf{x}, \mathbf{p})$ space using $v_k = \mu_{v_k} + u_k \sigma_{v_k}$ and used in the constraint function in Equation 1. This new constraint $g_j(\mathbf{v}^*)$ replaces the probabilistic constraint function in Equation 2 to avoid expensive simulations such as MCS.

Hybrid Mean Value (HMV) Method: We use a gradient-based hybrid mean value (HMV) method [16,41] to compute “most probable target point” (MPTP): \mathbf{u}_{HMV} . The gradient (\mathbf{n}_j) of the j -th constraint is computed at point (\mathbf{d}, \mathbf{u}) . The steps in HMV method to compute MPTP $(\mathbf{u}_{\text{HMV}})$ is provided as follows:

Step 1: Set iteration counter $t=0$, $t_{max} = T$, convergence parameter ε , Target Reliability Index β , and $\mathbf{u}_{\text{HMV}}^0 = [0]_{1 \times K}$.

Step 2: If $t \leq 2$, compute:

$$\mathbf{n}_j(\mathbf{u}_{\text{HMV}}^t) = -\frac{\nabla_{\mathbf{u}} g_j(\mathbf{d}, \mathbf{u}_{\text{HMV}}^t)}{\|\nabla_{\mathbf{u}} g_j(\mathbf{d}, \mathbf{u}_{\text{HMV}}^t)\|_2}; \quad \mathbf{u}_{\text{HMV}}^{t+1} = \beta \cdot \mathbf{n}_j(\mathbf{u}_{\text{HMV}}^t). \quad (4)$$

Step 3: If $t > 2$, compute the convexity estimate of g_j as follows:

$$\zeta_{\text{HMV}}^t = (\mathbf{n}_j(\mathbf{u}_{\text{HMV}}^t) - \mathbf{n}_j(\mathbf{u}_{\text{HMV}}^{t-1})) \cdot (\mathbf{n}_j(\mathbf{u}_{\text{HMV}}^{t-1}) - \mathbf{n}_j(\mathbf{u}_{\text{HMV}}^{t-2})). \quad (5)$$

Step 4: If $\zeta_{\text{HMV}}^t > 0$, that is, g_j is convex at \mathbf{d} , compute $\mathbf{u}_{\text{HMV}}^{t+1}$ using Equation 4.

Step 5: Else, $g_j(\mathbf{u}_{\text{HMV}}^t)$ is concave at point \mathbf{d} , compute:

$$\mathbf{u}_{\text{HMV}}^{t+1} = \beta \cdot \frac{\mathbf{n}_j(\mathbf{u}_{\text{HMV}}^t) + \mathbf{n}_j(\mathbf{u}_{\text{HMV}}^{t-1}) + \mathbf{n}_j(\mathbf{u}_{\text{HMV}}^{t-2})}{\|\mathbf{n}_j(\mathbf{u}_{\text{HMV}}^t) + \mathbf{n}_j(\mathbf{u}_{\text{HMV}}^{t-1}) + \mathbf{n}_j(\mathbf{u}_{\text{HMV}}^{t-2})\|_2}. \quad (6)$$

Step 6: If $|g_j(\mathbf{u}_{\text{HMV}}^{t+1}) - g_j(\mathbf{u}_{\text{HMV}}^t)| < \varepsilon$, **Stop**. Else, $t = t + 1$.

Step 7: If $t \leq T$, go to **Step 3**. Else **Stop**.

Based on convexity check in Step 3 using Equation 5, HMV switches between Advanced Mean Value (AMV) method in Step 4 and Conjugate Mean Value (CMV) method in Step 5. Hence, HMV benefits from properties of the both AMV and CMV methods; and can handle convex and moderately non-linear concave functions [21]. Readers are referred to [41] for further details on HMV.

3.2 Preference-based Evolutionary Multi-objective Optimization

Using PMA for reliability estimation in optimization formulation defined in Equation 2, ReF can be computed. However, computing the complete ReF is computationally costly. The proposed approach suggests using any R-EMO algorithm [37] to incorporate the DM's objective preferences to evaluate a part of the ReF that satisfies their criteria.

In the current work, R-NSGA-III [32] is used as an R-EMO algorithm. The procedure for computing the reference points in R-NSGA-III is provided in Figure 2. It takes user-defined reference points ($\bar{r}^{(k)}$), population per reference point,

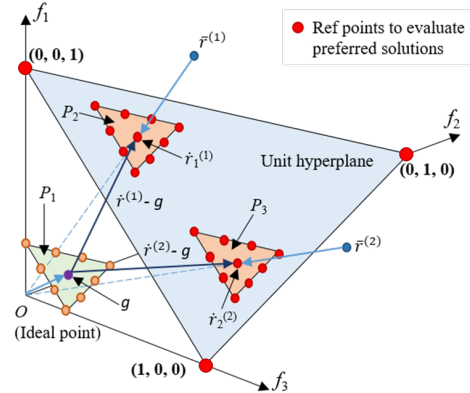


Fig. 2. A sketch of the R-NSGA-III's reference point computation procedure [37]. $\bar{r}^{(1)}$ and $\bar{r}^{(2)}$ are two reference points provided by DM. P_1 is the shrunk hyperplane depending on parameter μ . P_2 and P_3 are reference planes on unit hyperplane corresponding to the DM preferences $\bar{r}^{(1)}$ and $\bar{r}^{(2)}$. $\hat{r}^{(1)}$ and $\hat{r}^{(2)}$ are the intercept of unit hyperplane and normalized reference point vectors $\bar{r}^{(1)}$ and $\bar{r}^{(2)}$. Extreme reference points are also included for finding extreme PF solutions along with preferred solutions.

and shrinkage factor (μ) as input and generates reference points (red dots) on a unit hyperplane. μ controls the spread of MCDM solutions. Additionally, M extreme points on the unit simplex are supplied for the R-NSGA-III to focus on the extreme PO solutions for a better objective normalization purpose. The extreme solutions allow to locate the ideal point (O), which is used to translate shrunk reference points from O towards $\bar{r}^{(k)}$ on the unit simplex. These

translated reference points are then used to find preferred ReMCDM points by R-NSGA-III.

Table 1. Problem description for ReMCDM. N, M , and G denote the number of variables, objectives, and constraints, respectively. R_P is the reference point(s) used to compute ReMCDM solutions.

Example	# Variables (N)	# Objectives (M)	# Constraints (G)	# Reference Points (R_P)	Reference Point(s) (R_P)
Benchmark 1	2	2	1	1	[0.4, 1.8]
Benchmark 2	2	2	2	2	[0.9, 6], [0.6, 8]
I-Beam	4	2	1	2	[300, 0.035], [600, 0.015]
Welded Beam	4	2	4	1	[15, 0.006]
Disc Brake	4	2	4	2	[5, 2], [3, 3]
Two Bar Truss	3	2	3	2	[0.065, 8000], [0.085, 5000]
Car Side Impact	7	3	10	1	[40, 4.0, 60]
WATER	3	5	7	1	$\mathbf{z}^{nad} = [8.267e4, 1.349e3, 2.853e6, 1.597e7, 3.747e4]$

4 Results

The proposed approach for ReMCDM computation is implemented on 2 benchmark and 6 real-world engineering applications. The description of the benchmark and real-world engineering examples are outlined in Table 1. PF and ReF are evaluated by executing NSGA-II [11] for 100 generations with a population size of 100. ReMCDM solutions are evaluated by executing the R-NSGA-III [32] algorithm for 100 generations, and the population size per reference point is fixed at 20 for bi-objective, 21 for three-objective, and 35 for five-objective example. The GA parameters i.e. simulated binary crossover: SBX (cross-over probability $p_c=1.0$ and crossover operator $\eta_c=30$) and polynomial mutation: PM (mutation probability $\eta_m=30$) are kept the same for all examples. The HMV method is implemented with a maximum iterations ($T=100$) and a convergence parameter ($\varepsilon = 10^{-4}$) as the termination criteria, whichever is reached first.

4.1 Benchmark Examples

The details for Benchmark Example 1 and the uncertainty associated with the variables are provided below:

$$f_1(\mathbf{x}) = x_1^2 + x_2^2, \quad f_2(\mathbf{x}) = (x_1 - 1)^2 + (x_2 - 1)^2, \quad g(\mathbf{x}) = x_1^2 + x_2^2 - 1 \leq 0,$$

$$\mathbf{x} \sim N(\mu_{\mathbf{x}}, 0.2), \quad [\mathbf{x}^{lb}, \mathbf{x}^{ub}]_i = [0, 1]. \quad i = 1, 2.$$

This is a bi-objective problem having two uncertain design variables and one constraint. Figure 3(a) represents PF in black dots; and ReF in blue, green, and magenta dots, corresponding to reliability indices $\beta=2.0$, $\beta=3.0$, and $\beta=4.0$,

respectively. Note that two extreme points of the ReF is also found to provide stability in estimating the ideal point O . It can be observed that the ReF is a part of PF shifted towards the higher values of f_2 leaving out the lower f_2 as infeasible solutions for accommodating the variable uncertainty while handling the reliability constraint. As the target reliability increases from 2.0 to 4.0 the ReF (being the part of PF) shifts toward the higher f_2 values.

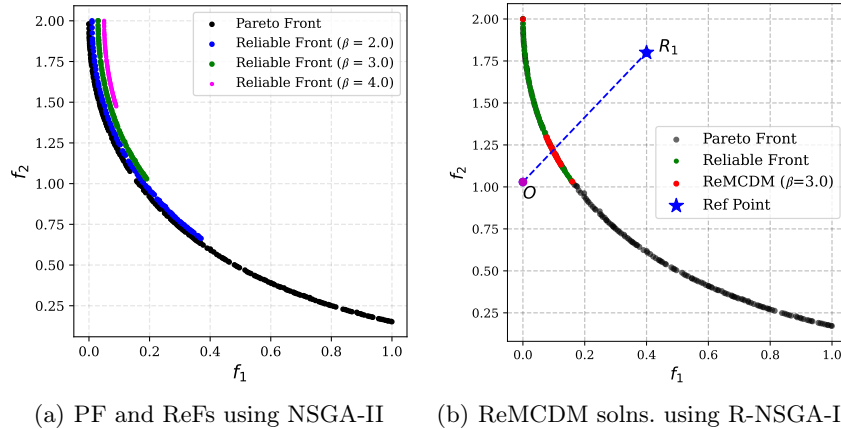


Fig. 3. Benchmark Example 1: (a) Scatter plot of Pareto front (black dots) and reliable front at different values of $\beta=[2.0, 3.0, 4.0]$ highlighted in blue, green, and magenta dots, respectively. Although ReFs lie on top of each other, ReFs are plotted with a slight shift to show clearly the extent of the respective fronts. (b) Reliability-based MCDM using reference point R_1 . Black and green dots represent PF and ReF, respectively. The red dots are ReMCDM solutions, which must always be a part of ReF. Point O is the ideal point of ReF.

Figure 4(a) presents the scatter plot of Pareto solutions in black dots and reliable solutions (blue, green, and magenta) in the design space at different target reliability indices (2.0, 3.0, and 4.0). It can be observed that as the target reliability index (β) increases, the reliable solutions move away farther from the constraint boundary. The adjacent color bar suggests that the reliable solutions shrink towards the region corresponding to higher f_2 and lower f_1 values. Figure 3(b) presents the ReMCDM solutions in red dots obtained using R-NSGA-III. Considering R_1 as a reference point with shrinkage factor ($\mu=0.25$), R-NSGA-III is executed for 100 generations to obtain part of the reliable front.

The details for Benchmark Example 2 and the uncertainty associated with the variables are provided in [8]. This is a bi-objective problem with two uncertain design variables and two constraints [8].

Figures 4(b) and 5(a) represent deterministic Pareto solutions and reliable solutions in design space and objective space, respectively. Figure 4(b) suggests that the Pareto solutions are located at the constraint boundary. As the target reliability index is increased from 2.0 to 4.0 the reliable solutions shift inside the feasible space to accommodate the variable uncertainty and to satisfy the

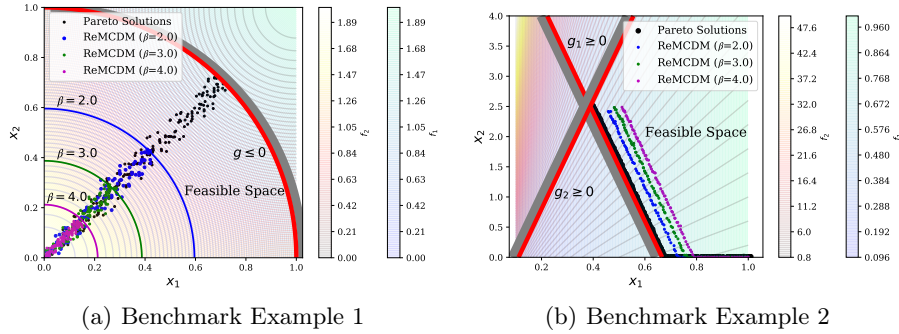


Fig. 4. Benchmark Examples: Pareto optimal front (black dots) and reliable fronts (ReFs) at different values of $\beta = [2.0, 3.0, 4.0]$ are highlighted in blue, green, and magenta dots, respectively. Here, the fronts are not deliberately shifted, rather they are naturally shifted due to higher clearances needed from the constraint boundaries to achieve a higher reliability index. The contour plots for f_1 and f_2 with color legends shown on the right of the figures indicate the conflicting behavior of two objectives.

reliability constraints. Similarly, it can be observed from Figure 5(a) that a part of the ReF shifts inside the objective space. As the target reliability index increases from 2.0 to 4.0, the extent of the shifting in objective space also increases. Two reference points R_1 and R_2 (see Table 1) with shrinkage factor ($\mu=0.1$) are provided by the DM to execute the R-NSGA-III for evaluating the ReMCDM solutions. In Figure 5(b), the ReMCDM solutions are highlighted in red dots. It is to be noted that in this example the ReMCDM solutions are not part of PF, instead, they are shifted inside the objective space and lie on ReF.

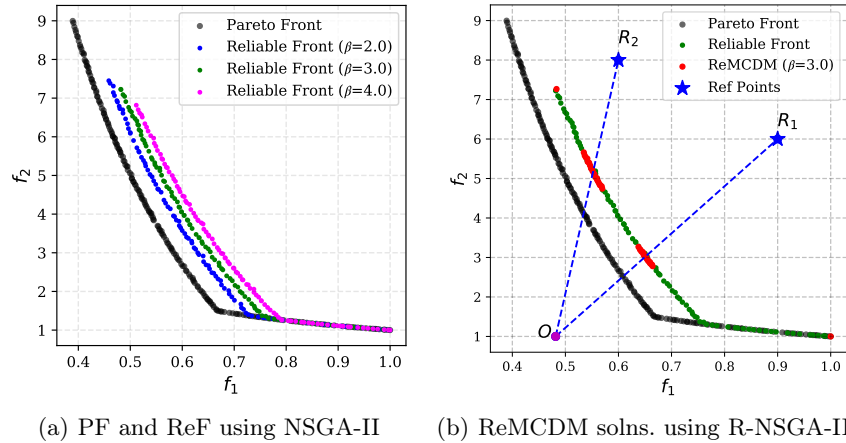


Fig. 5. Benchmark Example 2: (a) Pareto front (black points) and reliable fronts at different values of $\beta = [2.0, 3.0, 4.0]$ (colored points). (b) Reliability-based MCDM using reference points R_1 and R_2 . Black and green dots represent PF and ReF, respectively. Red dots are ReMCDM solutions.

4.2 Real-world Engineering Examples

The proposed approach is demonstrated on 5 real-world engineering examples- (i) I-beam design [21], (ii) Welded beam design [21], (iii) Disc brake design [21], (iv) Two-bar truss design [31], (v) Car side impact problem [31], and (vi) WATER problem [31]. The details of these real-world engineering examples are listed in Table 1.

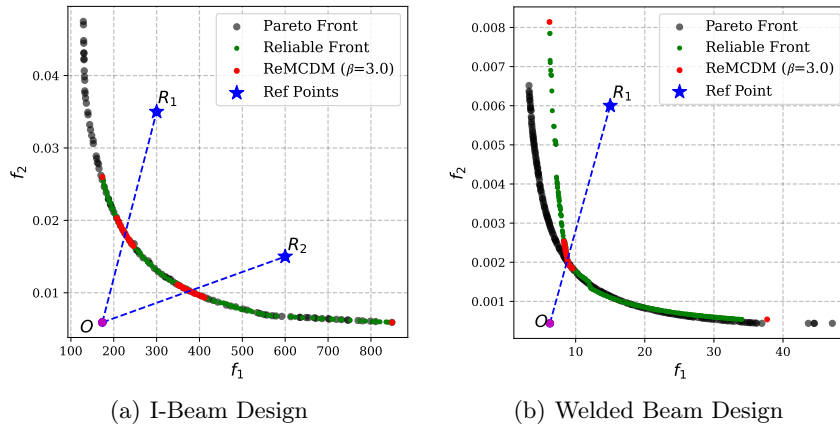


Fig. 6. Real-world problems: Black, green, and red dots represent PF, ReF, and ReMCDM solutions, respectively.

For the I-beam design example, target reliability index is set to $\beta=3.0$ and the uncertainty in the variable is expressed in terms of standard deviation $\sigma_{\mathbf{x}} = 0.2$ for each variable. Figure 6(a) presents the PF, ReF, and ReMCDM solutions for this problem. PF and ReF solutions are highlighted in black and green dots, respectively. It can be observed that the PF is reliable for small values of f_2 , but for small values of f_1 , the PF is not reliable. With the shrinkage factor fixed to $\mu=0.15$, two reference points R_1 and R_2 are supplied as input to the R-NSGA-III algorithm to evaluate the ReMCDM solutions. The ReMCDM solutions for reference points R_1 and R_2 are highlighted in red dots. It is important to highlight that to obtain the preferred reliable solutions (red points), the original PF or complete ReF (green points) are not required to be found. They are shown here to demonstrate the working of our proposed ReMCDM approach.

In welded beam design example, variable uncertainty is defined as $\sigma_{\mathbf{x}} = 0.25$ for each variable, and target reliability index β is set to 3.0. Figure 6(b) highlights the PF and ReF for this problem. For lower values of f_2 , ReF is the part of PF. However, for smaller values of f_1 , the ReF deviates from the PF to make solutions more reliable. ReMCDM solutions for reference point R_1 are computed using R-NSGA-III algorithm with a shrinkage factor of $\mu = 0.2$. A part of the ReMCDM solutions belongs to PF, whereas a part is shifted away from the PF.

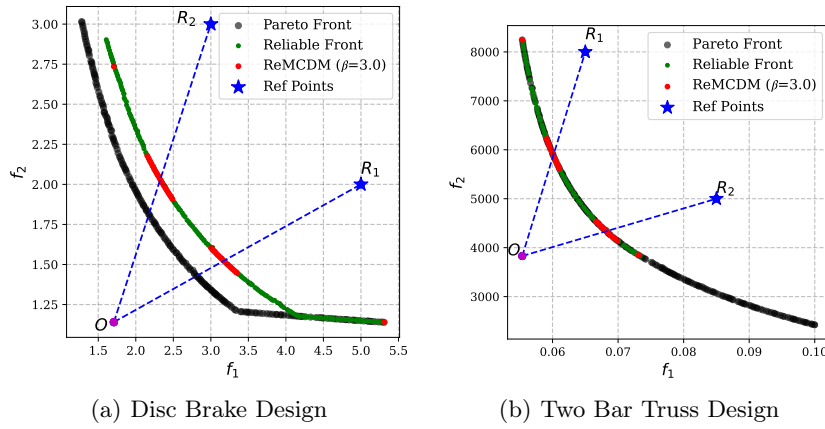


Fig. 7. Real-world Examples: Black, green, and red dots represent PF, ReF, and ReMCDM solutions, respectively. For two bar truss problem, ReF, shown with green points, spans about the left half of the PF.

The result of the disc brake example is presented in Figure 7(a). PF and ReF are highlighted in black and red color dots, respectively. The target reliability index $\beta = 3.0$ is used for this problem. The variable uncertainty in terms of standard deviation is defined as $\sigma_{\mathbf{x}} = [1.0, 1.0, 5.0, 1.0]$. A part of ReF and PF coincides at lower values of f_2 , whereas for higher f_2 values ReF shifts away from the PF. Two reference points R_1 and R_2 are used to compute the ReMCDM solutions using the R-NSGA-III algorithm ($\mu = 0.15$). Figure 7(b) presents the result for two bar truss example. Variable uncertainty in terms of standard deviation $\sigma_{\mathbf{x}} = [0.0025, 0.0025, 0.25]$ is used for this problem. In this example, ReF is a part of PF which corresponds to small values of f_1 (< 0.073 units). Two reference points R_1 and R_2 are used to compute the ReMCDM solution using R-NSGA-III algorithm. The shrinkage factor $\mu = 0.15$ is used.

Figure 8 represents the PF, ReF, and ReMCDM solutions for the car side impact example. The target reliability index $\beta = 3.0$ is used for this problem. Further details for this example are presented in Table 1. The variable uncertainty for this example is defined as $\sigma_{\mathbf{x}} = 0.1$, for each variable. The PF is represented by black points, and the ReF is shown with green points. Some parts of the ReF are dominated by the PF, while other parts of the ReF overlap with the PF. With shrinkage factor value set at $\mu =$

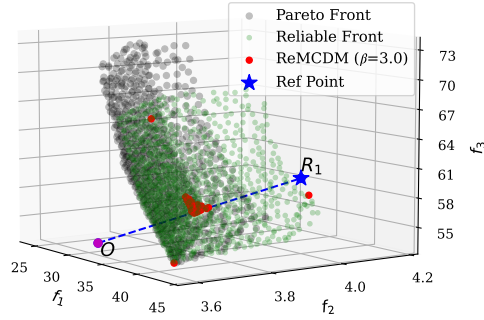


Fig. 8. Car Side Impact Example: Scatter plot indicates Pareto front (black dots) and reliable front at $\beta = 3.0$ (green dots). The ReMCDM solution corresponding to reference point R_1 is highlighted in red dots.

0.1 and population per reference point set as 21, the R-NSGA-III algorithm is used to compute the ReMCDM solutions for reference point R_1 . It is noteworthy to find the preferred reliable points (shown in red points), the original PF (black) or complete ReF (green) are not required to be found.

Next, we consider a five-objective WATER example [31]. This example has three design variables and seven constraints. Further description of this problem is provided in [31]. The results of the WATER example are presented in Figure 9. The gray, cyan, and orange lines depict Pareto front, reliable front, and ReMCDM solutions, respectively. The black line indicates the ideal preferred point (IPP) obtained at the intersection point of reliable front and line joining the reference point and ideal point. The objective function values in the plots are normalized according to the range of the objective function values in PF. In this example, the reference point (R_1) is chosen as the nadir point of ReF. Figure 9 indicates that ReF is a part of PF. The objective function f_5 values of PF are shrunk to obtain the ReF. A slight shrinkage in the objective $f_1, f_2,$ and f_3 is also observed from the figure.

To compute the reliable front and ReMCDM solutions, the target reliability index value of $\beta = 3.0$ is used. The variable uncertainty for this example is defined as $\sigma_{\mathbf{x}} = 0.02$, for each decision variable. Further algorithmic details for this example are presented in Table 1. To compute the ReMCDM solution, reference point R_1 (provided in Table 1) is supplied by the DM. The R-NSGA-III parameters used are shrinkage factor ($\mu = 0.15$) and population per reference point ($R_p = 35$). The proposed bi-level ReMCDM approach computes the preferred reliable points (orange line), without computing the original PF (gray line) or complete ReF (cyan line) significantly reducing the computational cost in terms of objective function and constraint function evaluations.

5 Conclusions

In this paper, we have proposed a Reliability-based Multi-criteria Decision-making (ReMCDM) approach to effectively address the challenges of solving constrained multi/many-objective optimization problems (M/MaOPs) under variable uncertainties and having objective preferences. By integrating the DM's

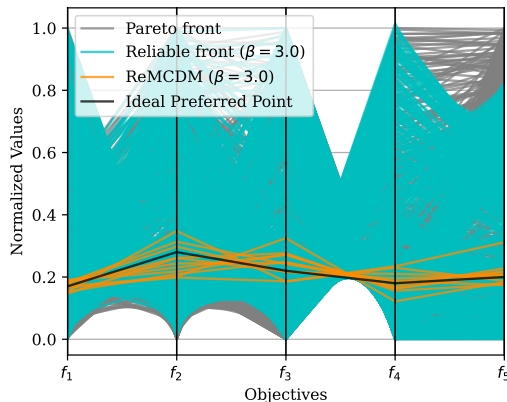


Fig. 9. WATER Example: Parallel coordinate plot indicates Pareto front (gray lines) and reliable front at $\beta = 3.0$ (cyan lines). The ReMCDM solutions corresponding to reference point (R_1) are highlighted in orange lines. The black line indicates ideal preferred point computed as the intersection of reliable front with the line joining reference point and ideal point.

preferences and utilizing the Hybrid Mean Value (HMV) method for constraint handling, ReMCDM has provided a computationally efficient way to obtain the most relevant part of the Reliable front (ReF), rather than computing the entire ReF and finding any part of the original Pareto-optimal front (PF). This approach has shown to be effective in benchmark and real-world applications, paving the way for future research in a combined task of constraint handling, preference incorporation, and decision-making under uncertainty.

In future studies, the performance of R-EMO algorithms including R-NSGA-III, R-NSGA-II, C-TAEA, and RVEA can be compared for the ReMCDM task using the updated \hat{R} -HV metric proposed in another study [38]. As the current approach requires computation of the reliability index (β) at each design point in every generation, it is associated with relatively high computational cost. Utilizing machine learning based reliability estimation methods can further decrease the computational cost of the ReMCDM task [27,39]. Literature on small failure probability i.e. sampling-based, surrogate-based, and statistics of extreme-based approaches can be used for small failure probability studies [17]. Visualization plays a vital role in assisting DMs in providing their preferences and choosing the final solution. The ReMCDM framework can be integrated with an appropriate visualization technique for interactive decision-making on a reliable front [34,36]. Though the proposed approach discusses constraint handling under uncertain variables, the robustness of objective function [37,35] can be integrated to obtain a combined robust and reliable decision-making framework.

Source Code Availability

The source code on benchmark examples discussed in the current paper is available in the following GitHub link: <https://github.com/deepanshuITM/ReMCDM>.

References

1. Aoues, Y., Chateaneuf, A.: Benchmark study of numerical methods for reliability-based design optimization. *Structural and multidisciplinary optimization* **41**(2), 277–294 (2010)
2. Bhattacharjee, K.S., Singh, H.K., Ryan, M., Ray, T.: Bridging the gap: Many-objective optimization and informed decision-making. *IEEE Transactions on Evolutionary Computation* **21**(5), 813–820 (2017)
3. Chankong, V., Haimes, Y.Y.: *Multiobjective decision making: theory and methodology*. Courier Dover Publications (2008)
4. Cheng, R., Jin, Y., Olhofer, M., Sendhoff, B.: A reference vector guided evolutionary algorithm for many-objective optimization. *IEEE Transactions on Evolutionary Computation* **20**(5), 773–791 (2016)
5. Cho, T.M., Lee, B.C.: Reliability-based design optimization using convex approximations and sequential optimization and reliability assessment method. *Journal of mechanical science and technology* **24**, 279–283 (2010)
6. Coello, C.A.C., Lamont, G.B., Van Veldhuizen, D.A., et al.: *Evolutionary algorithms for solving multi-objective problems*, vol. 5. Springer (2007)

7. Deb, K.: Multi-objective optimisation using evolutionary algorithms: an introduction. In: Multi-objective evolutionary optimisation for product design and manufacturing, pp. 3–34. Springer (2011)
8. Deb, K., Gupta, S., Daum, D., Branke, J., Mall, A.K., Padmanabhan, D.: Reliability-based optimization using evolutionary algorithms. *IEEE transactions on evolutionary computation* **13**(5), 1054–1074 (2009)
9. Deb, K., Kumar, A.: Light beam search based multi-objective optimization using evolutionary algorithms. In: 2007 IEEE Congress on Evolutionary Computation. pp. 2125–2132. IEEE (2007)
10. Deb, K., Kumar, A.: Interactive evolutionary multi-objective optimization and decision-making using reference direction method. In: Proceedings of the 9th annual conference on Genetic and evolutionary computation. pp. 781–788 (2007)
11. Deb, K., Pratap, A., Agarwal, S., Meyarivan, T.: A fast and elitist multiobjective genetic algorithm: NSGA-II. *IEEE transactions on evolutionary computation* **6**(2), 182–197 (2002)
12. Deb, K., Sundar, J.: Reference point based multi-objective optimization using evolutionary algorithms. In: Proceedings of the 8th annual conference on Genetic and evolutionary computation. pp. 635–642 (2006)
13. Habib, A., Singh, H.K., Ray, T.: A study on the effectiveness of constraint handling schemes within efficient global optimization framework. In: 2016 IEEE Symposium Series on Computational Intelligence (SSCI). pp. 1–8. IEEE (2016)
14. Jain, H., Deb, K.: An evolutionary many-objective optimization algorithm using reference-point based nondominated sorting approach, part II: Handling constraints and extending to an adaptive approach. *IEEE Transactions on evolutionary computation* **18**(4), 602–622 (2013)
15. Jaszkiwicz, A., Słowiński, R.: The ‘Light Beam Search’ approach—an overview of methodology applications. *European Journal of Operational Research* **113**(2), 300–314 (1999)
16. Keshtegar, B., Hao, P.: A hybrid self-adjusted mean value method for reliability-based design optimization using sufficient descent condition. *Applied Mathematical Modelling* **41**, 257–270 (2017)
17. Lee, I., Lee, U., Ramu, P., Yadav, D., Bayrak, G., Acar, E.: Small failure probability: principles, progress and perspectives. *Structural and Multidisciplinary Optimization* **65**(11), 326 (2022)
18. Li, G., Meng, Z., Hu, H.: An adaptive hybrid approach for reliability-based design optimization. *Structural and Multidisciplinary Optimization* **51**, 1051–1065 (2015)
19. Li, K., Chen, R., Fu, G., Yao, X.: Two-archive evolutionary algorithm for constrained multiobjective optimization. *IEEE Transactions on Evolutionary Computation* **23**(2), 303–315 (2018)
20. Meng, Z., Li, G., Wang, B.P., Hao, P.: A hybrid chaos control approach of the performance measure functions for reliability-based design optimization. *Computers & Structures* **146**, 32–43 (2015)
21. Meng, Z., Li, G., Wang, X., Sait, S.M., Yıldız, A.R.: A comparative study of metaheuristic algorithms for reliability-based design optimization problems. *Archives of Computational Methods in Engineering* **28**, 1853–1869 (2021)
22. Meng, Z., Yıldız, B.S., Li, G., Zhong, C., Mirjalili, S., Yıldız, A.R.: Application of state-of-the-art multiobjective metaheuristic algorithms in reliability-based design optimization: a comparative study. *Structural and Multidisciplinary Optimization* **66**(8), 191 (2023)
23. Miettinen, K.: Nonlinear multiobjective optimization. In: International series in operations research and management science (1998)

24. Miettinen, K., Mäkelä, M.M.: On scalarizing functions in multiobjective optimization. *OR spectrum* **24**, 193–213 (2002)
25. Molina, J., Santana, L.V., Hernández-Díaz, A.G., Coello, C.A.C., Caballero, R.: g-dominance: Reference point based dominance for multiobjective metaheuristics. *European Journal of Operational Research* **197**(2), 685–692 (2009)
26. Neumann, F., Neumann, A., Singh, H.K.: Evolutionary computation for stochastic problems. In: *Proceedings of the Genetic and Evolutionary Computation Conference Companion*. pp. 1352–1368 (2024)
27. Pannerselvam, K., Yadav, D., Ramu, P.: Scarce Sample-Based Reliability Estimation and Optimization Using Importance Sampling. *Mathematical and Computational Applications* **27**(6), 99 (2022)
28. Ray, T., Singh, H.K., Isaacs, A., Smith, W.: Infeasibility driven evolutionary algorithm for constrained optimization. *Constraint-handling in evolutionary optimization* pp. 145–165 (2009)
29. Singh, H.K., Branke, J.: Identifying stochastically non-dominated solutions using evolutionary computation. In: *International Conference on Parallel Problem Solving from Nature*. pp. 193–206. Springer (2022)
30. Steuer, R.E.: *Multiple criteria optimization: Theory, computation and applications*. Wiley (1986)
31. Tanabe, R., Ishibuchi, H.: An easy-to-use real-world multi-objective optimization problem suite. *Applied Soft Computing* **89**, 106078 (2020)
32. Vesikar, Y., Deb, K., Blank, J.: Reference point based NSGA-III for preferred solutions. In: *2018 IEEE symposium series on computational intelligence (SSCI)*. pp. 1587–1594. IEEE (2018)
33. Wu, Y.T., Millwater, H., Cruse, T.: Advanced probabilistic structural analysis method for implicit performance functions. *AIAA journal* **28**(9), 1663–1669 (1990)
34. Yadav, D., Nagar, D., Ramu, P., Deb, K.: Visualization-aided multi-criteria decision-making using interpretable self-organizing maps. *European Journal of Operational Research* **309**(3), 1183–1200 (2023)
35. Yadav, D., Ramu, P., Deb, K.: Finding Robust Solutions for Many-Objective Optimization Using NSGA-III. In: *2023 IEEE Congress on Evolutionary Computation (CEC)*. pp. 1–8. IEEE (2023)
36. Yadav, D., Ramu, P., Deb, K.: Interpretable self-organizing map assisted interactive multi-criteria decision-making following Pareto-Race. *Applied Soft Computing* **149**, 111032 (2023)
37. Yadav, D., Ramu, P., Deb, K.: Multi-objective Robust Optimization and Decision-Making Using Evolutionary Algorithms. In: *Proceedings of the Genetic and Evolutionary Computation Conference*. pp. 786–794 (2023)
38. Yadav, D., Ramu, P., Deb, K.: An updated performance metric for preference-based evolutionary multi-objective optimization algorithms. In: *Proceedings of the Genetic and Evolutionary Computation Conference*. pp. 612–620 (2024)
39. Yadav, D., Sekar, K., Ramu, P.: Adaptive sampling based estimation of small probability of failure using interpretable self-organising map. *Structural Safety* **109**, 102470 (2024)
40. Yang, D., Li, G., Cheng, G.: Convergence analysis of first order reliability method using chaos theory. *Computers & structures* **84**(8-9), 563–571 (2006)
41. Youn, B.D., Choi, K., Du, L.: Adaptive probability analysis using an enhanced hybrid mean value method. *Structural and Multidisciplinary Optimization* **29**, 134–148 (2005)
42. Youn, B.D., Choi, K.K.: Selecting probabilistic approaches for reliability-based design optimization. *AIAA journal* **42**(1), 124–131 (2004)

43. Youn, B.D., Choi, K.K., Du, L.: Enriched Performance Measure Approach for Reliability-Based Design Optimization. *AIAA journal* **43**(4), 874–884 (2005)
44. Youn, B.D., Choi, K.K., Park, Y.H.: Hybrid analysis method for reliability-based design optimization. *J. Mech. Des.* **125**(2), 221–232 (2003)
45. Zhang, Q., Li, H.: MOEA/D: A multiobjective evolutionary algorithm based on decomposition. *IEEE Transactions on evolutionary computation* **11**(6), 712–731 (2007)